J. Anat. (2002) **200**, pp431–438

Investigation of a cyclopic, human, term fetus by use of magnetic resonance imaging (MRI)

D. Situ,[1] C. W. Reifel,[1] R. Smith,[2] G. W. Lyons,[1] R. Temkin,[1] C. Harper-Little[2] and S. C. Pang[1]

[1]*Departments of Anatomy and Cell Biology, Queen's University, Kingston, Ontario, Canada K7L 3N6*
[2]*Diagnostic Radiology, Queen's University, Kingston, Ontario, Canada K7L 3N6*

Abstract

Using magnetic resonance imaging (MRI), the internal neural and craniofacial malformations of a cyclopic fetus are described. External facial features were characterized by a tubular proboscis situated above a single eye slit. The brain was recognized as 'pancake' type alobar holoprosencephaly (a condition where the undifferentiated telencephalon partially surrounds a monoventricle). Displacement of some bones that normally contribute to the orbit could be clearly discerned. Absence of neural structures (e.g. falx cerebri, corpus callosum) and missing components of the ethmoid bone indicated a midline deficit. This correlates with proposed theories of cyclopic embryopathy, which suggest that the prechordal plate and the neural crest cells are affected during the third week of gestation in cyclopia.

Key words cyclopia; holoprosencephaly; magnetic resonance imaging.

Introduction

Cyclopia is a severe form of holoprosencephaly caused by failure of embryonic prosencephalon cleavage and differentiation (Wilson et al. 1989). There is an absence of olfactory tracts and septum pellucidum, while the prosencephalon remains as an undifferentiated sphere, rather than becoming hemispheric. In more severe forms of holoprosencephaly, the fronto-nasal process, calvaria and mid-facial structures may be deformed. In extreme cases, holoprosencephaly can take the form of cyclopia, in which the absence of mid-facial tissue results in one eye in a single orbit.

During the 1940s, 1950s and 1960s, the Department of Anatomy and Cell Biology, as part of the Queen's Medical School, acquired more than 75 human fetal specimens, including the cyclops fetus which is currently under study. The use of these fetuses for biomedical investigation was approved by the Office of the Chief Coroner of Ontario, Canada. Upon receipt of the fetus, only the external features were documented before it was preserved in formalin for storage. The non-invasive nature of MRI now allows visualization of internal structures without destroying the specimen, and thus can provide data to explain the defects of morphogenesis.

Correspondence
Dr Conrad W. Reifel, Department of Anatomy and Cell Biology, Faculty of Health Sciences, 9th Floor Botterell Hall, Queen's University, Kingston, Ontario, Canada K7L 3N6. Tel. (613) 533 2851; fax: (613) 533 2566; e-mail: cr2@post.queensu.ca

Accepted for publication *9 April 2002*

Materials and methods

The 21-year-old mother of the fetus did not suffer any illness (external or genetic) and had not taken any medication during the early stages of gestation. She had begun to pass amniotic fluid on the fifth day preceding delivery. The fetal heart stopped 7 h before parturition. A prior pregnancy had produced an infant without defect.

In a post-mortem examination, the male fetus was reported to have a crown foot length of 38.1 cm, with a single eye slit measuring 6.4 cm. The tubular proboscis was 2.5 cm long and 1.2 cm wide. Externally, the rib cage, thorax and abdomen were normal, but alternating polydactyly was observed on the left hand and right foot. The ears were low-set. (Fig. 1)

The magnetic resonance examination was performed on a GE 1.5 Tesla Signa scanner running on 5.4.2 software. Multislice, multiplane, T2 weighted sections were obtained using a 2D FSE technique with a slice thickness of 3 mm and interslice gap of 0.5 mm

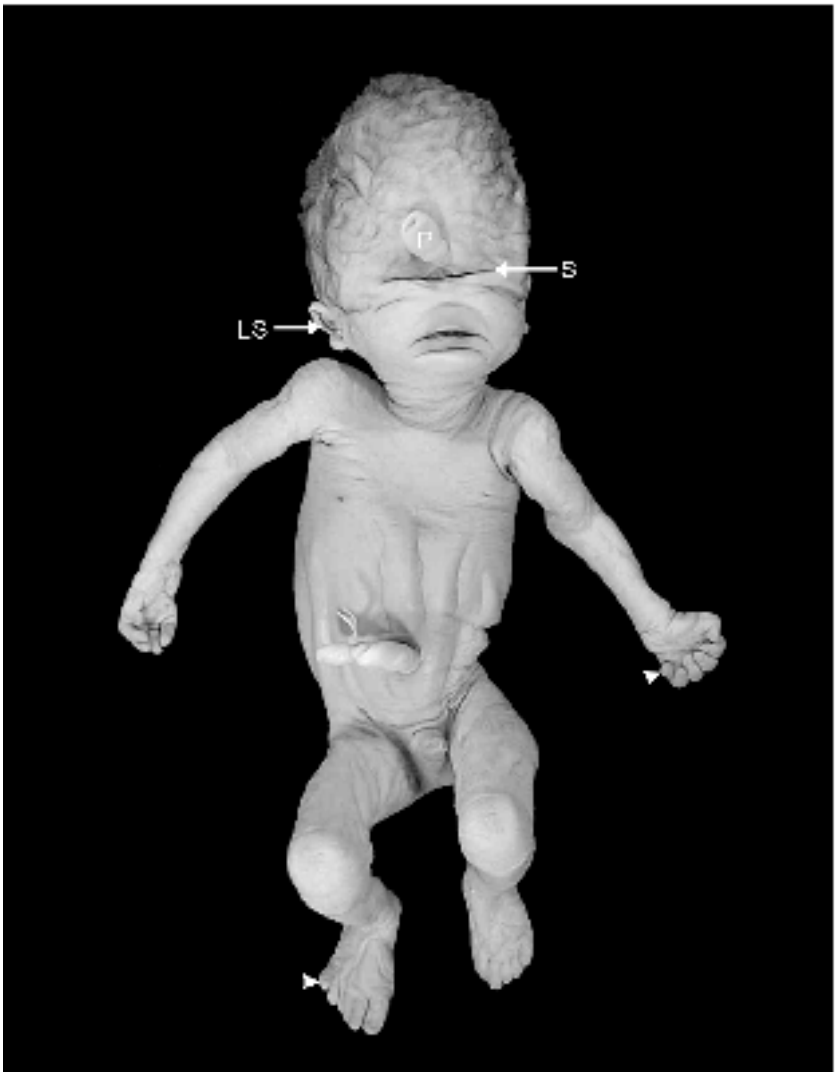

Fig. 1 External anomalies. Proboscis (P) is situated above a single eye slit (S). Alternating polydactyly (arrowheads) occurs on the left hand and right foot. The ears are low set (LS).

(256^2 matrix). Contiguous slices of 0.8 mm were obtained using a 3D SPGR technique (512^2 matrix). The voxel size ranged from 0.5 to 0.8 mm. Window and level parameters for each image were optimized to enhance tissue contrast.

Observations

In sagittal (Fig. 2) and axial (Fig. 3) MRI scans, the telencephalon appears as an undivided cerebrum that only partially covers the anterior surface of a single fused ventricle. The cerebrum is a thick mass that thins as it reaches the edges of its folds, characteristic of pancake alobar holoprosencephaly. The monoventricle is continuous with a large cyst that can be seen to occupy a large portion of the dorsal cranial cavity. In coronal sections (Fig. 4), a number of structures are absent: longitudinal fissure, falx cerebri, corpus callosum, third ventricle, septum pellucidum, olfactory bulbs and olfactory tracts. More caudally, a mass of undifferentiated nuclei is seen above the thalamus (Fig. 4).

Due to the fusion of the thalami, no third ventricle exists (Figs 4 and 5). Two primitive eye buds (Figs 2, 5 and 6) are continuous with optic nerves (Figs 2, 5 and 7) which converge into a single, large optic nerve (Figs 5 and 8) that enters the diencephalon at the level of the thalamus (Figs 2 and 5).

The proboscis is seen as a tubular structure that is rooted above the single eye slit externally (Fig. 1). Sagittal (Fig. 2) and coronal (Fig. 6) scans reveal the exact termination point of the proboscis as an ethmoid notch, a remnant of the rudimentary ethmoid, which forms part of the superior orbit above the two eye buds. The root of the proboscis contributes to the

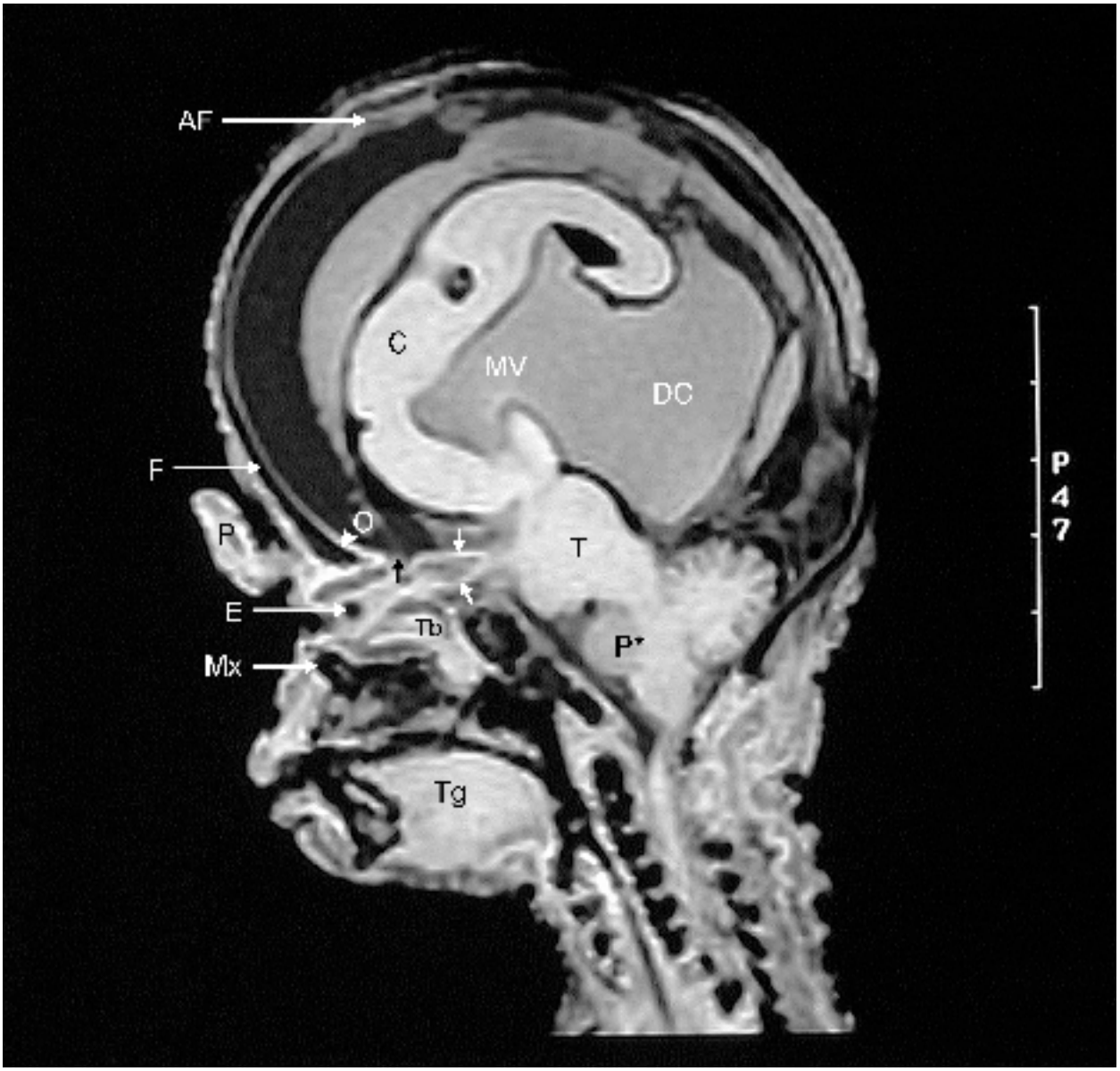

Fig. 2 Sagittal MRI of the head and neck. Cerebrum (C) partially covers the monoventricle (MV), which is continuous with a large dorsal cyst (DC). Corpus callosum is absent. Root of proboscis (P) terminates at the ethmoid notch (black arrow), which with orbital plate (O) of frontal bone (F) and turbinates (Tb) contributes to the superior aspect of the orbit containing the primitive eye buds (E). Maxilla (Mx) does not contribute to the inferior orbit. (AF, anterior fontanelle; P*, pons; T, thalamus; Tg, tongue; white arrows, optic nerve.)

superior medial roof of the orbit posterior to the orbital plate of the frontal bone (Fig. 2). The superior and middle turbinates make up the superior and lateral walls while the frontal bone forms the medial portion of the orbit. The greater and lesser wings of the sphenoid form the most inferior curvature of the single orbit (Fig. 7).

A single frontal bone (Fig. 3) extends posteriorly as far as the anterior fontanelle medially (Figs 2 and 8) and the coronal suture laterally (Fig. 5). Posterior to the latter, two parietal bones are separated by a sagittal suture. Due to the tilt of the specimen's head during scanning, the coronal sections in Figs 6–8 are oblique. As a result, the greater wing of the sphenoid, shown in Fig. 7, is seen in its most posterior position, where it begins its curve upward to meet the frontal bone of the orbit and appears superior to the eye buds that mark the centre of the orbit.

The inferior turbinates (Fig. 2) and maxilla (Figs 2 and 7) are structurally normal. What appears to be a

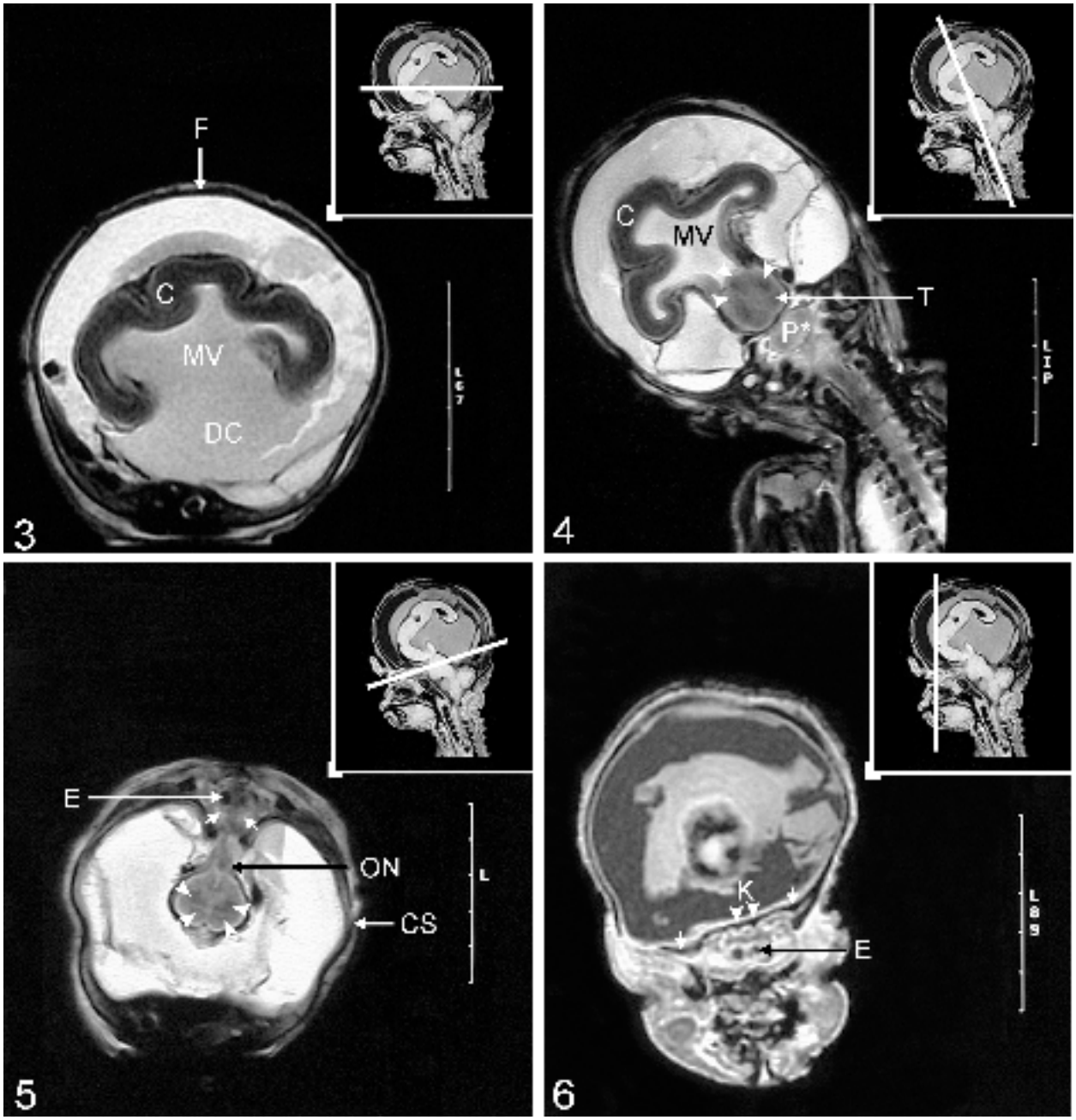

Fig. 3 Axial section. Undifferentiated cerebrum (C) covers the monoventricle (MV), which extends into the dorsal cyst (DC). F, frontal bone.

Fig. 4 Coronal section. Thalamus (T) sits above the pons (P*) and below a mass of nuclei (small arrowheads) which are in direct contact with the undivided folds of the cerebrum (C). Longitudinal fissure, falx cerebri, corpus callosum, third ventricle and septum pellucidum are absent.

Fig. 5 Axial section. Leading from each primitive eye bud (E) are two optic nerves (arrows) which converge to form a single optic nerve (ON) that enters the diencephalon. (CS, coronal suture; arrowheads, fused thalamic nuclei.)

Fig. 6 Coronal section. Ethmoid notch (K) marks the termination of the proboscis and contributes to the roof of the orbit containing the primitive eye buds (E). Due to the oblique tilt of the specimen, the posterior portions of the greater wings of the sphenoid (arrows) are observed above the primitive eye buds.

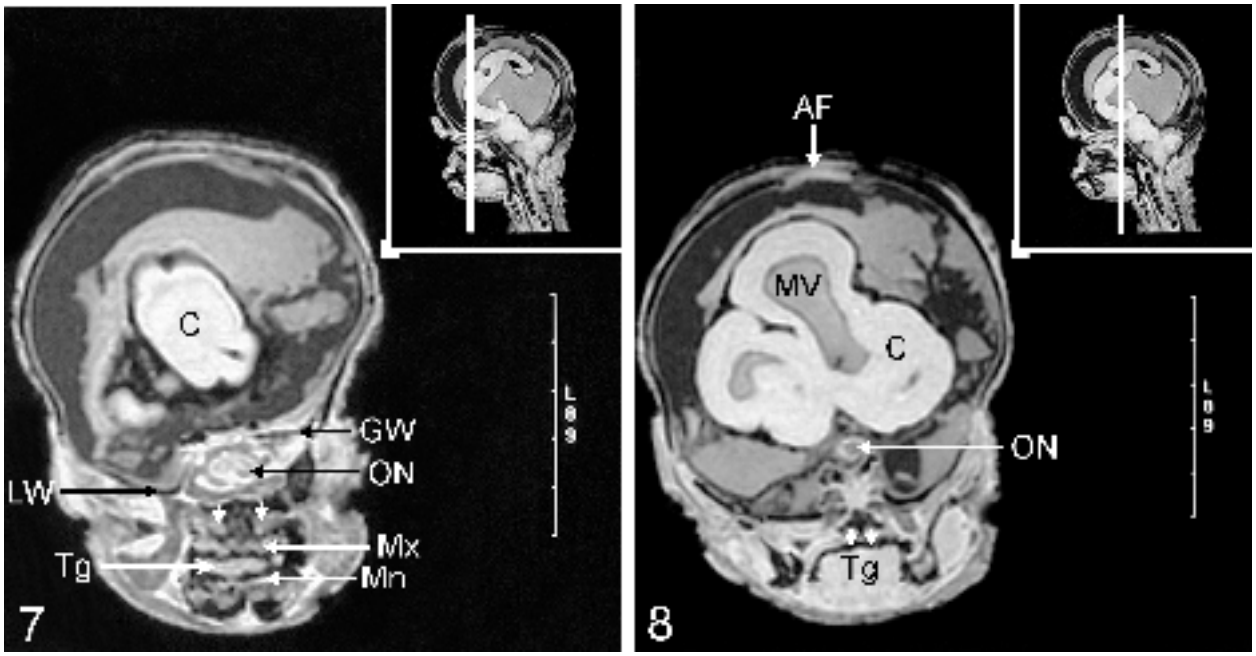

Fig. 7 Coronal section. Maxilla (Mx) and mandible (Mn) are structurally complete. Lesser wings of sphenoid (LW) form part of the floor of the single orbit. Due to the oblique tilt of the specimen, the posterior portions of the greater wings of the sphenoid (GW) are observed superior to the two optic nerves (ON). Inferior turbinates (arrows), situated in their normal position relative to the palatine processes of maxillae (Mx), do not make contact with any olfactory structures. C, cerebrum.
Fig. 8 Coronal section. Single optic nerve (ON) distal to the convergence of two optic nerves seen in Fig. 7. The palate (Pa) is structurally normal. AF, anterior fontanelle; Tg, tongue; MV, monoventricle.

rudimentary vomer is seen superior to the maxilla. However, the orbital surface of the maxilla has become displaced from its usual position, while the inferior turbinates have shifted downward and make no contact with the nasal region (Figs 2 and 7). The palate is structurally normal (Fig. 8), including a premaxillary component which contains the upper incisor teeth.

Discussion

The present investigation demonstrates that MRI is a valuable tool to determine the internal, anatomical defects of the malformed fetus, without the need of dissection.

Our MRI results confirm the developmental defects in the facial bones reported by dissections of cyclopic specimens (Souza et al. 1990; McGrath, 1992). Certain components of the ethmoid are missing, specifically the crista galli, perpendicular plate of the nasal septum and the ethmoid air sinuses. In order for the bone orientation of cyclopia to occur, the superior and middle turbinates must shift upward in order to lie in the postero-superior wall of the orbit (just underneath the rim of the orbital plate); the maxilla, vomer and inferior turbinates become detached and the parts of the orbital complex that are usually taken up by the maxilla become replaced by the downward shift of the fused greater and lesser wings of the sphenoid (contributing the entire lower curvature of the single orbit) and the medially fused zygomatic arches (composing the lower rim).

There is histological documentation that the proboscis is composed of epithelium, nerve and musculature that are indicative of the nasal capsule. McGrath (1992) has stated that the proboscis may be the antero-superior part of the nasal cavity developed in the absence of medial components such as the presphenoid, perpendicular plate of the ethmoid, cristi galli and septal cartilage. Kjaer et al. (1991) have noted that the proper formation of the sphenoid bones and the nasal capsule (which will later contribute to the ethmoid bone) is dependent on the integrity of the prechordal mesoderm.

Observations taken from numerous cyclopic specimens, each in varying stages of development, have identified portions of the medial nasal swelling as missing (Kjaer et al. 1991). Structures that arise from the lowermost portion of the medial nasal swelling, such as the premaxilla, may therefore be absent as well. If

enough material is lacking, cleft lip may accompany the usual list of cyclopic external defects. The lateral nasal swellings therefore fuse in the midline to surround a single, central nostril observed in cebocephaly. In the more severe case of ethmocephaly (or cyclopia) both the lateral and the medial nasal swellings are diminished and the remaining tissue continues to proliferate to form the tubular proboscis (Cohen et al. 1971; McGrath, 1992). However, other studies imply that the single undulated nasal placode is secondary to the absence of the interplacodal area, the space where the missing medial, nasal swelling would have formed. Mazzola et al. (1990) and Vermeij-Keers (1990) state that without this area, agenesis of the premaxillae, nasal septum, nasal lacrimal bones and ethmoid will ensue.

The olfactory placodes (at the end of the fourth week of normal development) deepen to form the nasal cavity, which normally extends toward the cranial cavity floor. The tissue surrounding this area will later become the nasal capsule. Absence of the presphenoid, a centre of ossification between the lesser wings which will later give rise to the anterior body of the sphenoid (Souza et al. 1990), will cause a failure of the intended postero-inferior deflection of the expanding cavity towards the nasopharynx. Instead, the postero-superior part of the nasal capsule will develop a sphenoidal conchal element, which will fill the posterior portion of the ethmoid notch. Finally, with the lack of a nasal septum to anchor the nasal components to the upper jaw, the outcome is a distal, mobile face appendage (proboscis) commonly situated above the eyes (McGrath, 1992). Hence, in most cases and in this specimen, the maxillary and vomer bones are present, but as completely separate structures.

The absence of the nasal cartilage will create disturbances in the formation of the basicranial skeleton and the subsequent abnormal, partial, osseous fusion of facial bones. These abnormalities of the face and basal cranium are both consequences of the early embryonic defects, which may include a direct effect of defective sonic hedgehog (SHH) signalling on migrating neural crest cells as well as the deficiency of anterior midline structures (Alghren & Bronner-Fraser, 1999).

Many reports have emphasized that it is not the mere fusion of elements due to missing median structures that is responsible for the cyclopic phenotype (O'Rahilly & Muller, 1989). Extensive studies using the zebrafish model have proposed that the single fused retinas observed in cyclopic mutants are due to failure of primordial eye field separation during gastrulation (Varga et al. 1999). Within the early neural plate, diencephalic precursors are situated postero-medially to the primordial plate eye field and must move anteriorly to form the ventral diencephalon (the future hypothalamus). As a result of this anterior migration or shift of cells, the eye field becomes separated into left and right eyes. Mutants with single retinas fused across the midline will result if this ventral region of the diencephalon fails to form and the single eye field remains an undisturbed layer (Varga et al. 1999). The single, medial layer of optic primordia may have also contributed to the failed descent of the nasal capsule (Cohen et al. 1971). Yet timing of the onset of morphologically detectable abnormality may affect the outcome. Cyclopia *sensu stricto* (one median eye in a single orbit) occurs after onset of abnormal development at week $2^1/_2$, which at 3 weeks results in cyclopia *sensu lato* (paired ocular structures in a single orbit, synopthalmia; O'Rahilly & Muller, 1989).

The prosencephalon consists of two parts: the telencephalon, from which the primitive cerebral hemispheres arise, and the diencephalon. Since the diencephalon partially differentiates into recognizable fused thalamic nuclei, it is expected that the globus pallidus, hypothalamus and optic stalk may have also partially developed in our specimen. Due to the fusion of the thalami and the loss of the third ventricle, no communication with the cerebral aqueduct and fourth ventricle occurs and hence the protruding posterior cyst of the CSF results (Barkovich, 2000).

Within the literature, there is a general agreement that in cyclopia, a disturbance to the rostral end of the notochord mesoderm must have occurred during the 3rd week of gestation in order to encompass the wide array of neural and facial anomalies (Cohen et al. 1971; Kjaer et al. 1991; Roessler & Muenke, 1998). Some go further to postulate that a deficiency of prechordal plate material (and hence a developmental field defect) may be the localized neural induction deficit (Corsello et al. 1990; Liu et al. 1997; Varga et al. 1999). More recently, Jin et al. (2001) have emphasized the importance of anterior visceral endoderm (AVE) and prechordal mesoderm involvement for proper anterior patterning during the primitive streak stage of development in embryos.

The prechordal mesoderm ensures that the median neural plate cells down regulate the retinal precursor

gene expression so that these cells proliferate to form the ventral diencephalon (Sampath et al. 1998; Varga et al. 1999). An absence in this signalling will lead to the improper differentiation of these cells, so that the median neural plate cells instead develop into retinal precursors and merge with the single, fused retinal field. In addition, the prechordal plate is stated to stimulate the prosencephalon to divide and migrate laterally, so that a deficiency in prechordal plate material will decrease induction of forebrain growth and development (Varga et al. 1999). A decrease in forebrain matter not only produces the alobar holoprosencephalic brain, but also will decrease the forebrain's production of SHH growth factor (Hu & Helms, 1999; Muller et al. 2000). *Shh* expression has been documented in the axial mesoderm, ventral neural tube and the organizer (Muller et al. 2000). Because SHH is essential to neural crest cell survival, a decrease in *Shh* expression may lead to neural crest cell death (Ahlgren & Bronner-Fraser, 1999). Since neural crest cells have been found to provide positional information for the fetal facial midline (Hu & Helms, 1999), their depletion has produced defects in forebrain, cyclopia or microophthalmia and reduced or absent jaw structures (Ahlgren & Bronner-Fraser, 1999). Prechordal plate also functions inductively in stimulating the normal development of the nose and central facial skeleton (Varga et al. 1999).

The expression of *Shh* is essential for normal development of the floor plate and ventral brain (Muller et al. 2000). Winged-helix gene *HNF3*β and homeobox gene *Otx2* are hypothesized to be regulators of *Shh* expression in the mouse model. Both genes are expressed in the AVE and prechordal mesoderm. Jin et al. (2001) created double heterozygous mutant *Otx2*+/–; *HNF3*β+/– mice and observed reduced *Shh* expression in the anterior midline correlating with varying degrees of holoprosencephaly, cyclopia with proboscis-like structures and anterior forebrain truncations.

More recently, X-ray-based computer tomography (CT) has gained favour for developmental studies (Goodman & Gorlin, 1983; Johnson, 1989). Because the cyclops specimens either die prenatally or live, on average, 4 h after birth, the bones of the skull have not completed their ossification, which makes accurate viewing by X-ray alone, even when compiled in three-dimensional images, difficult. This is especially relevant when the main structures of interest are the bones of the orbit, nasal region and the maxilla.

By use of non-invasive MRI, developing bone as well as cartilaginous structures can be studied and the specimens can be retained for future observations. Morphological details can be attained with this method at accuracy equivalent to that of dissection while still preserving the fetus. In addition, with MRI, one can establish a better comprehension of relative structural positions, in three dimensions, which is lost in studies with dissection.

Acknowledgment

We wish to thank the Advisory Research Committee, Queen's University, for financial support of this project.

References

Ahlgren SC, Bronner-Fraser M (1999) Inhibition of sonic hedgehog signaling in vivo results in craniofacial neural crest cell death. *Current Biol*. **9**, 1304–1314.

Barkovich JA (2000) *Pediatric Neuroimaging*, 3rd edn, pp. 318–324. Philadelphia: Lippincott, Williams & Wilkins.

Cohen MM Jr, Jirasek JE, Guzman RT, Gorlin RJ, Peterson MQ (1971) Holoprosencephaly and facial dysmorphia: nosology, etiology and pathogenesis. *Birth Defects* **7**, 125–135.

Corsello G, Buttitta P, Cammarata M, Presti AL, Maresi E, Zumpani L, Giuffre L (1990) Holoprosencephaly: examples of clinical variability and etiologic heterogeneity. *Am. J. Med. Genet*. **37**, 244–249.

Goodman RM, Gorlin RJ (1983) *The Malformed Infant and Child. An Illustrated Guide*, pp. 60–61. New York: Oxford University Press.

Hu D, Helms JA (1999) The role of Sonic Hedgehog in normal and abnormal craniofacial morphogenesis. *Development* **126**, 4873–4884.

Jin O, Harpal K, Ang SL, Rossant J (2001) *Otx2* and *HNF3*β genetically interact in anterior patterning. *Int. J. Dev. Biol*. **45**, 357–365.

Johnson VP (1989) Holoprosencephaly: a developmental field defect. *Am. J. Med. Genet*. **34**, 258–264.

Kjaer I, Keeling JW, Graem N (1991) The midline craniofacial skeleton in holoprosencephalic fetuses. *J. Med. Genet*. **28**, 846–855.

Liu DPC, Burrowes DM, Qureshi MN (1997) Cyclopia: craniofacial appearance on MR and three-dimensional CT. *Am. J. Neuroradiol*. **18**, 543–546.

Mazzola R., Stricker M, Van Der Meulen J, Raphael B (1990) Evolving concepts in the understanding and treatment of craniofacial malformations. In *Craniofacial Malformations* (eds Stricker T, Van Der Meulen J, Raphael B, Mazzola R), pp. 27–60. Edinburgh: Churchill Livingstone.

McGrath P (1992) The proboscis in human cyclopia: an anatomical study in two dimensions. *J. Anat*. **181**, 139–149.

Muller F, Albert S, Blader P, Fischer N, Hallonet M, Strahle U (2000) Direct action of the nodal-related signal cyclops in

induction of sonic hedgehog in the ventral midline of the CNS. *Development* **127**, 3889–3897.

O'Rahilly R, Muller F (1989) Interpretation of some median anomalies as illustrated by cyclopia and symmelia. *Teratology* **40**, 409–421.

Roessler E, Muenke M (1998) Holoprosencephaly: a paradigm for the complex genetics of brain development. *J. Inherited Metabolic Dis*. **21**, 481–497.

Sampath K, Rubinstein AL, Cheng AMS, Liang JO, Fekang K, Solnica-Krezel LS, et al. (1998) Introduction to the zebrafish ventral brain and floorplates requires cyclops/nodal signaling. *Nature* **139**, 185–189.

Souza JP, Siebert JR, Beckwith BJ (1990) An anatomic comparison of cebocephaly and ethmocephaly. *Teratology* **42**, 347–357.

Varga ZM, Wegner J, Westerfield M (1999) Anterior movement of ventral diencephalic precursors separates the primordial eye field in the neural plate and requires cyclops. *Development* **126**, 5533–5546.

Vermeij-Keers C (1990) Craniofacial embryology and morphogenesis: normal and abnormal. In *Craniofacial Malformations* (eds Stricker T, Van Der Meulen J, Raphael B, Mazzola R), pp. 1–11. Edinburgh: Churchill Livingstone.

Wilson WG, Shanks DE, Sudduth KW, Couper KA, McIlhenny J (1989) Holoprosencephaly and interstitial deletion of 2 (p2101p2109). *Am. J. Med. Genet*. **34**, 252–254.